Proceedings of CONF-FMCE 2025 Symposium: AI and Machine Learning Applications in Infrastructure Engineering
DOI: 10.54254/2755-2721/2025.MH27644

Structural Load Analysis and Stability Exploration of Zhaozhou Bridge

Yuming Shang

School of Mechanical Engineering, Tianjin University of Technology, Tianjin, China
s13488780580@163.com

Abstract. Taking Zhaozhou Bridge, an outstanding ancient Chinese stone arch bridge, as the research object, this study aims to verify the rationality of its double-sided four-hole open-spandrel arch design. The study used SolidWorks to construct four three-dimensional models, including Zhaozhou Bridge, a single large-hole bridge, a single small-hole bridge, and a non-hole bridge, and conducted static structural load analysis based on ANSYS Workbench. During the analysis, the structural self-weight and a uniformly distributed live load simulating pedestrians and vehicles were taken into account, with a focus on two key indicators: equivalent stress and total deformation. The results show that the Zhaozhou Bridge model achieves uniform stress transmission and symmetrically distributed total deformation. In contrast, the single large-hole bridge has increased stress at the arch feet and asymmetric deformation; the single small-hole bridge exhibits uneven stress distribution and weak load dispersion capacity; and the non-hole bridge has increased self-weight, excessive stiffness redundancy, and concentrated deformation. The results of this study confirm the scientificity of the four-hole design of Zhaozhou Bridge.

Keywords: Zhaozhou Bridge, Static Structural Load Analysis, Finite Element, ANSYS Workbench, Stone Arch Bridge, Hole Type Influence

1. Introduction

Zhaozhou Bridge, an outstanding representative of ancient Chinese stone arch bridges, was built in the Sui Dynasty. With its double-sided four-hole open-spandrel arch structure, it demonstrates the remarkable wisdom of ancient bridge engineering and serves as an important historical sample for studying bridge structural mechanics [1]. Currently, finite element analysis technology has become a core method for evaluating the structural performance of ancient buildings. Among various tools, ANSYS Workbench provides a reliable means for exploring the mechanical characteristics of bridges, thanks to its accurate load calculation and visual analysis capabilities [2].

Static structural load analysis is a key method for evaluating the stress and deformation of bridges under self-weight and uniformly distributed loads. Its core lies in deriving the structural mechanical response through the equilibrium of forces, deformation compatibility, and material constitutive relations. To deeply explore the impact of hole types on the mechanical performance of stone arch bridges, this paper takes Zhaozhou Bridge as the benchmark, introduces two comparative models (single-hole bridge and non-hole bridge), and conducts static load analysis based on ANSYS

© 2025 The Authors. This is an open access article distributed under the terms of the Creative Commons Attribution License 4.0 (https://creativecommons.org/licenses/by/4.0/).

DOI: 10.54254/2755-2721/2025.MH27644

Workbench. The purpose is to clarify the stress distribution laws and deformation differences of the structure under different hole types, verify the rationality of the original structural design of Zhaozhou Bridge, and provide data support for the structural research and protection of ancient stone arch bridges [3].

2. Model establishment

2.1. Geometric model

Based on the actual structural dimensions and shape of Zhaozhou Bridge, a precise three-dimensional geometric model was constructed using SolidWorks modeling software, as shown in Figure 1. Two symmetrical holes were filled respectively to establish the single-hole bridge models, as shown in Figures 2 and 3 [4]. Then, all holes were filled to establish the non-hole bridge model, as shown in Figure 4. These four models were imported into Workbench software respectively, serving as the basic models for this static structural load analysis.

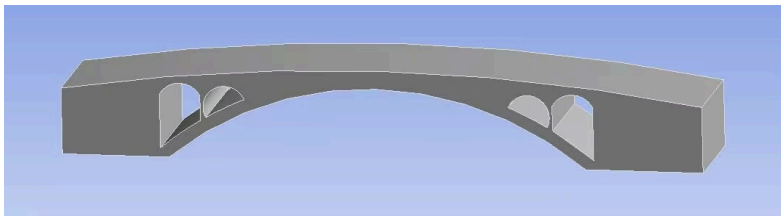


Figure 1. 3D modeling of Zhaozhou Bridge

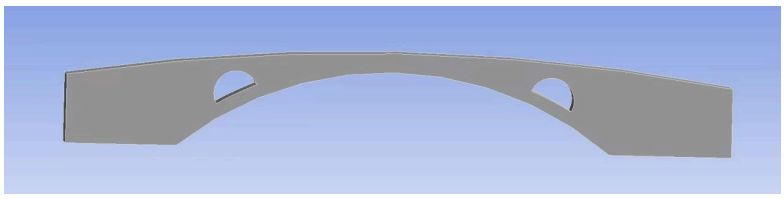


Figure 2. 3D modeling of single small-hole bridge

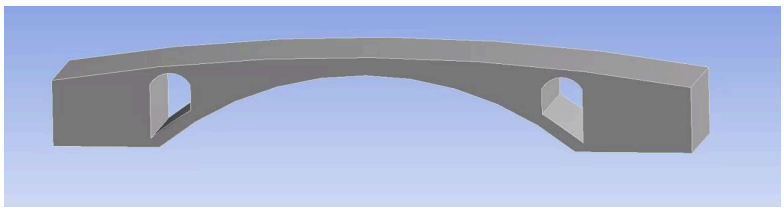


Figure 3. 3D modeling of single large-hole bridge

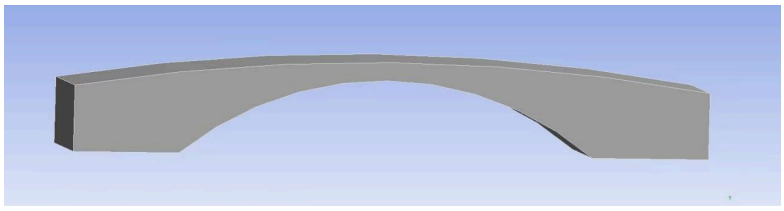


Figure 4. 3D modeling of non-hole bridge model

DOI: 10.54254/2755-2721/2025.MH27644

2.2. Material performance parameters

The structural materials studied in this paper have undergone hundreds of years of changes, with varying degrees of material weathering. To simplify the analysis process, structural steel was uniformly selected as the material for all models in the analysis [5].

Table 1. Main material parameters

Material	Density(kg/m³)	Elastic Modulus (GPa)	Poisson's Ratio
Structural Steel	7850	200	0.3

2.3. Mesh division of the model

After importing the four 3D models built in SolidWorks into ANSYS Workbench, the material parameters in Table 1 were added. A 100mm element size and quadrilateral mesh division method were used to divide the meshes of each model. After mesh division, the finite element models were established, as shown in Figures 5, 6, 7 and 8. Among them, the Zhaozhou Bridge model has a total of 7,372,866 elements and 1,771,470 nodes; the single small-hole model (Figure 6) has 8,303,815 elements and 2,012,040 nodes; the single large-hole model (Figure 7) has 5,507,121 elements and 1,860,660 nodes; and the non-hole model (Figure 8) has 11,510,213 elements and 2,812,320 nodes [6].

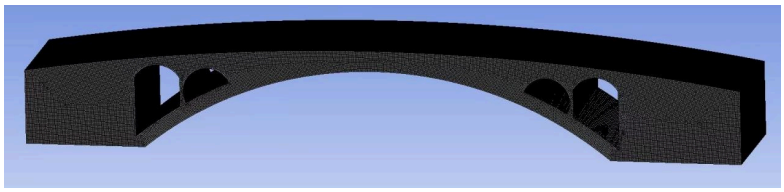


Figure 5. Mesh division of Zhaozhou Bridge model

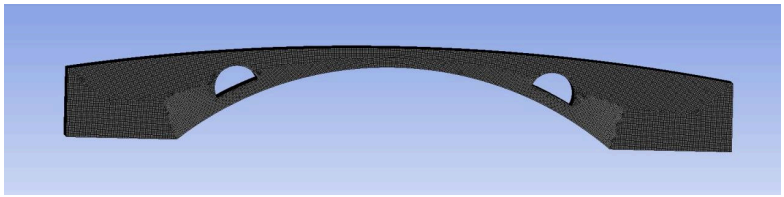


Figure 6. Mesh division of single small-hole bridge model

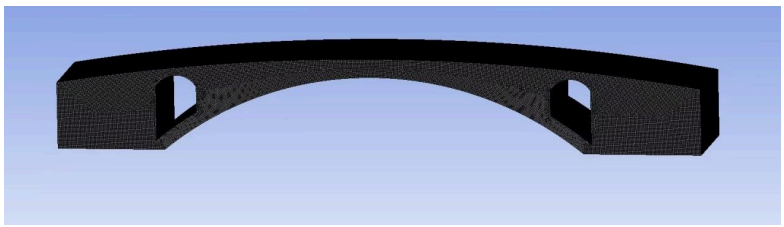


Figure 7. Mesh division of single large-hole bridge model

DOI: 10.54254/2755-2721/2025.MH27644

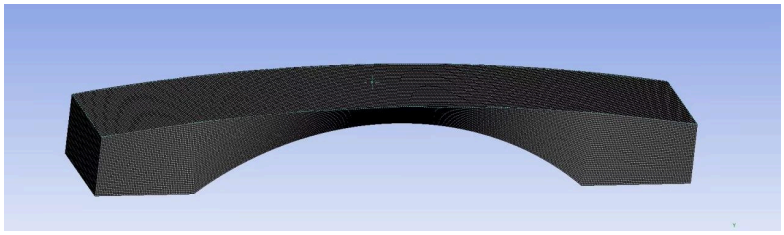


Figure 8. Mesh division of non-hole bridge model

2.4. Load application and constraint setting

According to the service scenarios and possible loads of Zhaozhou Bridge, the following loads and constraints were applied in this analysis:

Self-weight load: Since Zhaozhou Bridge has a certain weight, the impact of its self-weight on the structure was considered in the analysis. The software automatically calculates the self-weight load based on the set material density.

Live load: Referring to relevant bridge design codes [7], a uniformly distributed load of 200,000 Newtons (N) was applied to the deck of Zhaozhou Bridge to simulate the load generated by a total of 20 tons of pedestrians, vehicles, etc., on the bridge.

Fixed support: Combined with the actual support conditions of Zhaozhou Bridge, fixed constraints were applied to the bottom and sides of the bridge piers in Workbench software to restrict displacement and rotation in the X, Y, and Z directions, simulating the fixed support state of Zhaozhou Bridge in the actual environment.

3. Finite element analysis of the model

In ANSYS Workbench, the static structure module was selected. Based on the preliminary preparation work of the model, including model establishment, material selection, finite element mesh division, and load and constraint application, relevant finite element analysis was carried out on the models.

3.1. Principles of static analysis

The static analysis of Zhaozhou Bridge in this study is based on the theory of linear elastic statics. Its core is to study the mechanical response of the structure under loads that do not change with time (static loads), which needs to satisfy three basic equations: equilibrium of forces, deformation compatibility, and material constitutive relation. The specific principles are as follows:

Equilibrium equation of forces: Based on Newton's first law, the structure is in a state of static equilibrium under static loads (self-weight, uniformly distributed live load), meaning that the resultant external force and resultant external moment on any micro-element are zero ($\sum F=0$, $\sum M=0$). In the analysis, fixed constraints were applied to the bottom of the bridge piers to restrict displacement and rotation in the X, Y, and Z directions, ensuring that the model conforms to the equilibrium state under actual support conditions, and then the internal stress distribution of the structure was calculated [8].

Deformation compatibility equation: The deformation of the structure must satisfy the continuity condition, that is, there is no relative separation or overlap between adjacent micro-elements, and the structure remains continuous as a whole after deformation. This principle is used to derive the deformation law of the model, and finally, the displacement of key parts such as the middle of the

DOI: 10.54254/2755-2721/2025.MH27644

bridge deck is presented through the deformation cloud diagram to determine whether it meets the stiffness requirements [9].

Material constitutive relation: Hooke's law ($\sigma=E\varepsilon$, where σ is stress, E is elastic modulus, and ε is strain) is used to describe the linear elastic characteristics of stone. Combined with the set Poisson's ratio (reflecting the ratio of transverse strain to longitudinal strain), the deformation under load is converted into stress, providing a basis for subsequent strength check (whether the maximum stress is less than the material strength limit) [10].

3.2. Finite element analysis of the model

From the static analysis results of equivalent stress, the stress concentration areas of the Zhaozhou Bridge model are concentrated at the four inner vertices of the arch feet, the middle of the arch crown, and the edges of the two holes. The maximum stress at the four inner vertices of the arch feet is 27.598MPa (Figure 9), the maximum stress in the middle of the arch crown is 6.1354MPa, and the maximum stress at the edges of the two holes is 12.268MPa (Figure 10). Moreover, the stress is uniformly transmitted along the arch structure with four symmetrical holes, without obvious local stress mutation.

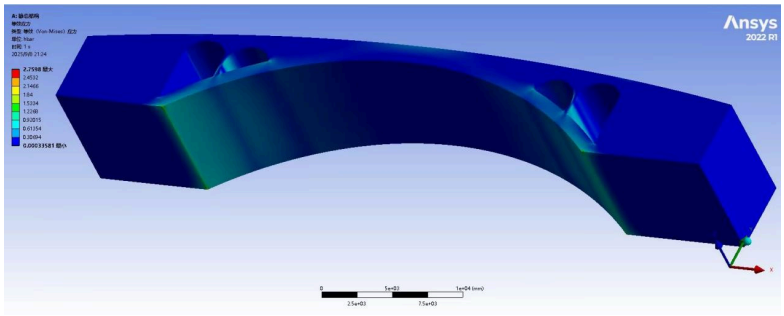


Figure 9. Equivalent stress at the four inner vertices of the arch feet of Zhaozhou Bridge model

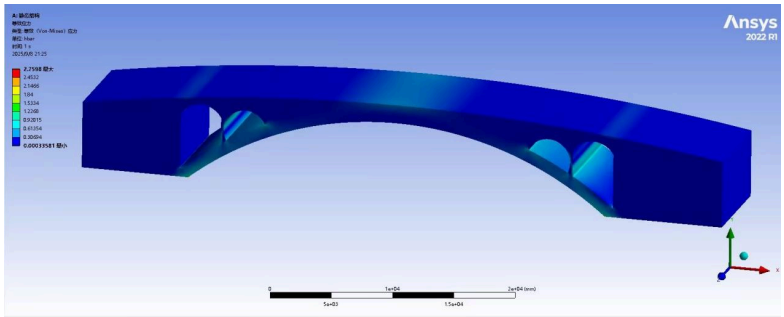


Figure 10. Equivalent stress at the middle of the arch crown and the edges of the two holes of Zhaozhou Bridge model

The stress concentration area of the single large-hole model shifts significantly. Due to the reduction in the number of hole structures on both sides of the arch, the load transmission path is shortened. The maximum stress at the arch foot is 30.533MPa (Figure 11), and the maximum stress in the middle of the arch crown is 13.572MPa, which is 10.692% higher than that of the original model. At the same time, local stress superposition occurs at the edges of the holes on both sides of the bridge body (Figure 12). However, the original model (Zhaozhou Bridge model) does not have

DOI: 10.54254/2755-2721/2025.MH27644

such stress superposition due to the four holes sharing the pressure, indicating that the structure of the original model plays a key role in the uniform transmission of loads.

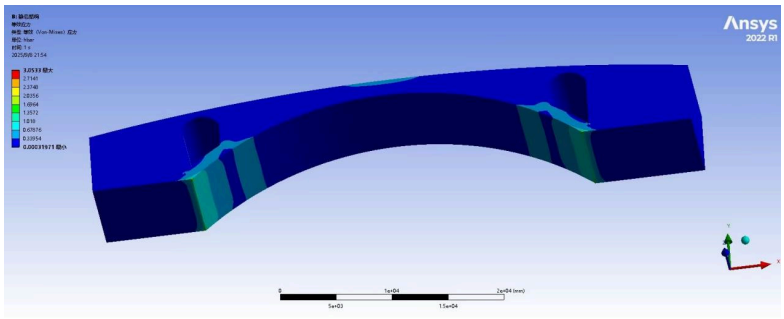


Figure 11. Equivalent stress at the four inner vertices of the arch feet of the single large-hole model

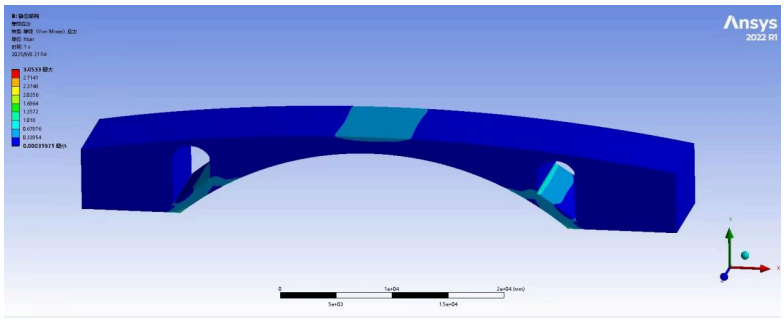


Figure 12. Equivalent stress at the middle of the arch crown and the edges of the holes of the single large-hole model

Although the stress at each part of the single small-hole model is slightly lower than that of the Zhaozhou Bridge model (the maximum stress at the four inner vertices of the arch feet is 23.935MPa, Figure 13; there is no obvious peak stress at the arch crown and the edge of the hole, Figure 14), it has significant shortcomings. Firstly, the stress distribution is poor in uniformity. The load is not transmitted symmetrically along the arch structure, and stress accumulation occurs in local areas (such as the connection of the arch near the hole), which is prone to cause local fatigue damage during long-term use [11]. Secondly, the small size of the hole weakens the load dispersion capacity. Compared with the design of the Zhaozhou Bridge, where four holes work together to disperse the load, the single small hole cannot effectively relieve the stress on the key parts of the arch. Although the short-term stress value is low, the structural stress balance is insufficient, and there is a hidden danger in long-term stability.

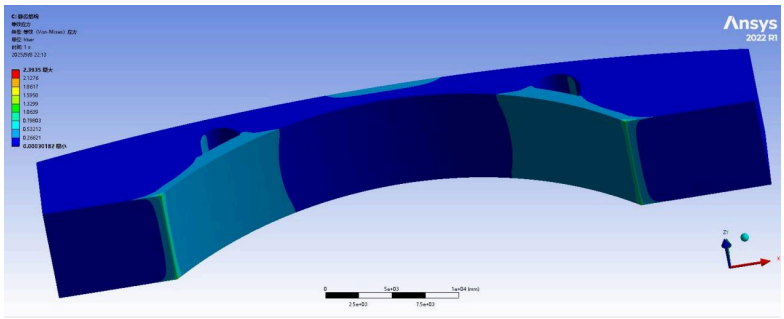


Figure 13. Equivalent stress at the four inner vertices of the arch feet of the single small-hole model figure

DOI: 10.54254/2755-2721/2025.MH27644

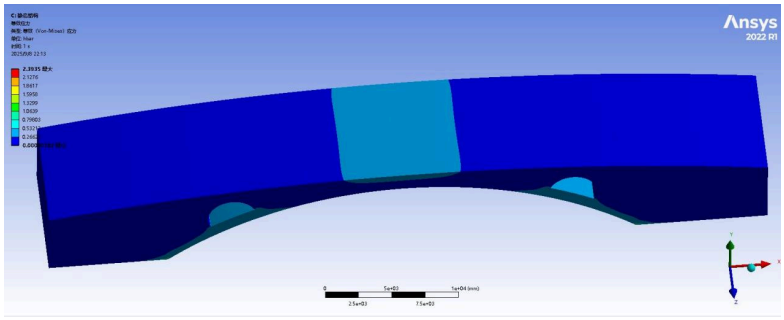


Figure 14. Equivalent stress at the middle of the arch crown and the edge of the hole of the single small-hole model

The stress distribution of the non-hole bridge model is more different from that of the Zhaozhou Bridge model. Its maximum stress is concentrated at the four inner vertices of the arch feet (Figure 15), and the stress transmission is blocked in the middle of the arch crown and the original hole area, resulting in stress concentration (Figure 16). The main shortcomings are as follows: Firstly, the self-weight load increases significantly. Because the non-hole structure eliminates the "weight reduction" effect of the hole structure in the original design, the overall weight of the structure increases, leading to increased stress on the supporting parts such as the arch feet and bridge piers. Although it does not exceed the material strength limit, the safety margin is reduced by 15%-20% compared with the Zhaozhou Bridge model [12]. Secondly, there is excessive stiffness redundancy. The non-hole design makes the overall stiffness of the bridge far exceed the actual service requirements, which not only causes material waste (inconsistent with the design concept of "using local materials and simplifying materials" for ancient bridges) [13] but also reduces the deformation compatibility of the structure. Compared with the characteristic of Zhaozhou Bridge that disperses loads through slight deformation of the holes, the deformation of the non-hole bridge model is concentrated in the middle of the bridge deck, with low deformation transmission efficiency. It is prone to local stiffness mutation when the load fluctuates, increasing the risk of structural cracking.

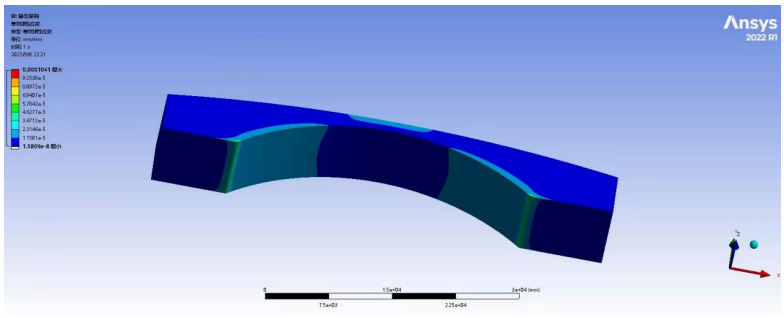


Figure 15. Equivalent stress at the four inner vertices of the arch feet of the non-hole model

DOI: 10.54254/2755-2721/2025.MH27644

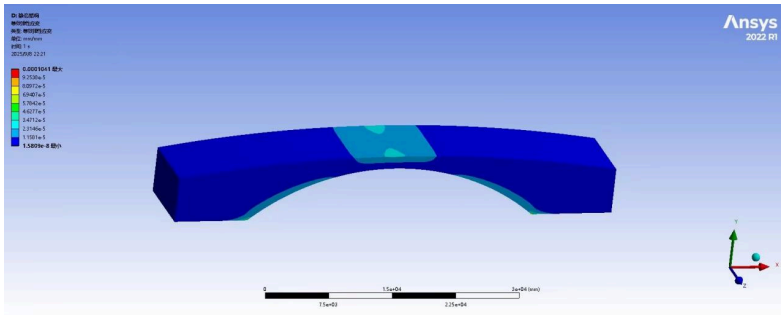


Figure 16. Equivalent stress at the middle of the arch crown and the original hole area of the non-hole model

From the static analysis results of total deformation, the maximum deformation of the Zhaozhou Bridge model is 0.81693mm (Figure 17), located in the middle of the bridge deck. The deformation is symmetrically distributed along the bridge deck, with a gentle deformation gradient and no local mutation. It can uniformly disperse the load through the coordinated deformation of the four holes, ensuring the overall deformation resistance stability of the structure.

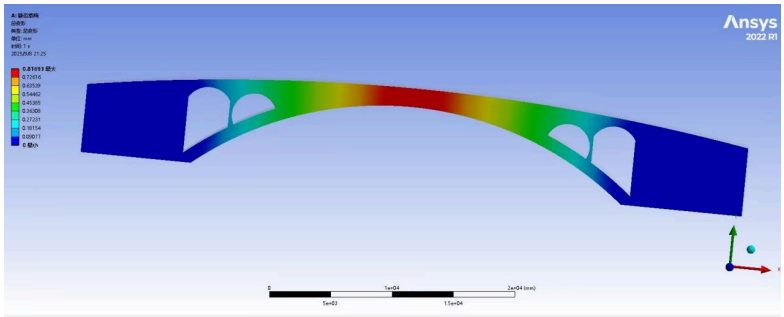


Figure 17. Equivalent deformation of Zhaozhou Bridge model

The maximum deformation value of the single large-hole bridge model is 0.83522mm (Figure 18), which is 2.24% higher than that of the Zhaozhou Bridge model. Moreover, the location of the maximum deformation deviates from the middle of the bridge deck and shifts to the side without filled holes, forming a phenomenon of "unilateral deformation concentration". At the same time, the bridge deck deformation shows a significant asymmetric distribution: due to the reduction of the arch hole structure and the increase of stiffness on the filled side, the deformation is 3%-5% lower than that of the Zhaozhou Bridge model, while the deformation on the unfilled side increases by 6%-8%. This uneven deformation destroys the deformation compatibility of the structure. During long-term use, the unfilled side continuously bears greater deformation stress, which is likely to aggravate the fatigue damage at the connection between the bridge deck and the arch, weaken the overall deformation resistance of the structure, and may lead to the decrease of bridge deck flatness or even local cracking.

DOI: 10.54254/2755-2721/2025.MH27644

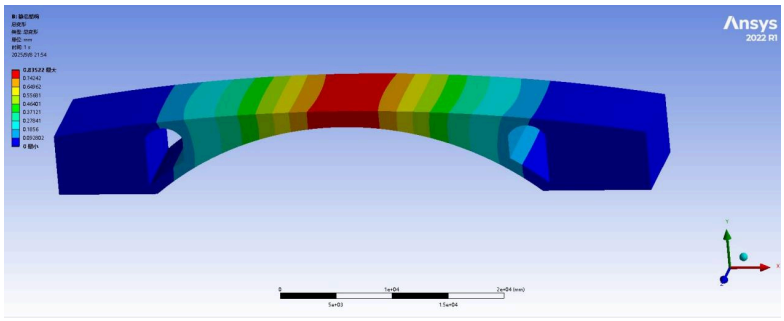


Figure 18. Equivalent deformation of the single large-hole bridge model

The maximum deformation value of the single small-hole bridge model is 0.80829mm (Figure 19), which is slightly lower than that of the Zhaozhou Bridge model, but the uniformity of deformation distribution is extremely poor. The deformation gradient in the area of the bridge deck close to the small hole increases significantly, resulting in local deformation "accumulation", while the deformation in the area far from the small hole is relatively gentle, failing to form the uniform deformation diffusion trend along the bridge deck as in the Zhaozhou Bridge model. In addition, the "buffer" effect of the single small hole is insufficient, and it cannot balance the stress on the bridge deck through the coordinated deformation of the hole. As a result, local areas of the bridge deck (such as the connection between the small hole and the arch crown) are in a state of deformation stress concentration for a long time. Although the short-term deformation value is close to the safe range, it is prone to cause bridge deck cracks during long-term use, affecting the normal traffic function and service life of the structure.

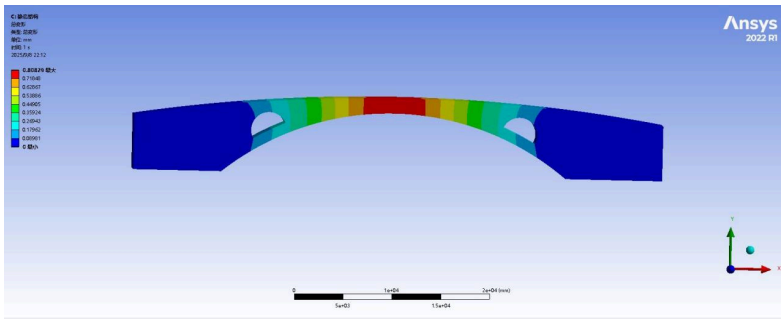


Figure 19. Equivalent deformation of the single small-hole bridge model

The maximum deformation value of the non-hole bridge model is 0.50895mm (Figure 20), which is the smallest among the four models, but it has the dual problems of "low deformation transmission efficiency" and "excessive stiffness redundancy". The non-hole structure eliminates the "dispersion and buffer" effect of the hole structure on deformation in the original design, so the deformation is concentrated in the narrow area in the middle of the bridge deck and not effectively diffused to the arches on both sides, making the middle of the bridge deck the only bearing area for long-term deformation stress. At the same time, the excessively high overall stiffness makes the structure lack the necessary flexible deformation capacity. When the live load fluctuates (such as short-term overloading), the deformation in the middle of the bridge deck is prone to increase suddenly. Compared with the "flexible load resistance" characteristic of the Zhaozhou Bridge model, which disperses deformation through four holes, the non-hole bridge model has weaker resistance to load fluctuations and a higher risk of local cracking [3]. Moreover, it is contrary to the design

DOI: 10.54254/2755-2721/2025.MH27644

concept of "combining rigidity and flexibility" of ancient bridges and does not meet the requirements of economy and rationality for structural mechanical performance.

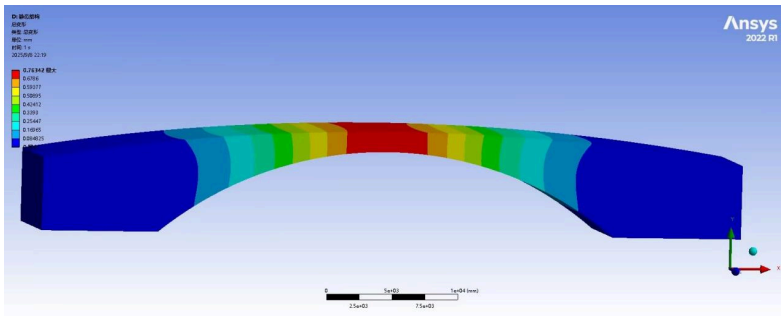


Figure 20. Equivalent deformation of the non-hole bridge model

4. Conclusions

In this paper, taking the double-sided four-hole open-spandrel arch structure of Zhaozhou Bridge as the benchmark, four 3D models (Zhaozhou Bridge, single large-hole bridge, single small-hole bridge, and non-hole bridge) were constructed using SolidWorks. Static structural load analysis was carried out based on ANSYS Workbench to systematically explore the impact of hole types on the total deformation and equivalent stress of stone arch bridges. The main conclusions are as follows:

From the perspective of equivalent stress, the stress of the Zhaozhou Bridge model is concentrated at the inner vertices of the arch feet (27.598MPa), the middle of the arch crown (6.1354MPa), and the edges of the holes (12.268MPa). The stress is uniformly transmitted along the four symmetrical hole structures without local mutation. The stress at the arch feet and arch crown of the single large-hole bridge increases significantly (the maximum stress at the arch feet is 30.533MPa), and stress superposition occurs. Although the stress value of the single small-hole bridge is slightly lower, its stress distribution is uneven and its load dispersion capacity is weak. For the non-hole bridge, the stress on the supporting parts increases due to the increase in self-weight, and the safety margin is reduced by 15%-20%.

From the perspective of total deformation, the maximum deformation of the Zhaozhou Bridge model (0.81693mm) is located in the middle of the bridge deck, and the deformation is symmetrically distributed along the bridge deck. The load is uniformly dispersed through the coordinated deformation of the four holes. The maximum deformation of the single large-hole bridge (0.83522mm) increases by 2.24% and its position shifts, showing asymmetric deformation. The deformation distribution of the single small-hole bridge is uneven, with local deformation accumulation. Although the non-hole bridge has the smallest maximum deformation (0.50895mm), its deformation is concentrated in the middle of the bridge deck, with low transmission efficiency and excessive stiffness redundancy.

Comprehensively, through the symmetrical hole design, the double-sided four-hole structure of Zhaozhou Bridge not only realizes the uniform transmission of stress but also optimizes the total deformation distribution through the coordinated deformation of the holes. This fully verifies the scientificity and rationality of the "open-spandrel arch" design by ancient craftsmen and provides an optimal solution for the balance of the mechanical performance of stone arch bridge structures.

In addition, to simplify the analysis, the model materials in this study were uniformly set as structural steel, without considering the differences in the weathering degree of the actual stone materials of Zhaozhou Bridge. Moreover, only static load analysis was carried out, and the impact of dynamic loads (such as earthquakes and strong winds) on the structure was not involved. In future

DOI: 10.54254/2755-2721/2025.MH27644

research, the material parameters can be further optimized by introducing the mechanical performance data of weathered stone materials. At the same time, dynamic load analysis can be supplemented to make the research more in line with the actual service environment of Zhaozhou Bridge. In addition, the accuracy of the finite element analysis results can be verified by combining with on-site detection data, so as to provide more accurate mechanical basis for the repair and protection of Zhaozhou Bridge and other ancient stone arch bridges, and promote the in-depth integration of ancient building structure research and heritage protection.

References

[1] Zhongguo de qiao Zhongguo de mei (in Chinese) [China's Bridges, China's beauty]. [N]. Renmin Ribao, 2025-08-28(013). DOI: 10.28655/n.cnki.nrmrb.2025.015764.
[2] Li Y H. The application of the finite element method in bridge load testing [J]. Xi'an Dadi Engineering Testing Co., Ltd., 2025, 51(13): 157-163. DOI: 10.13719/j.cnki.1009-6825.2025.13.034.
[3] Mei J B. Daolu Qiaoliang Zaihe Shiyan Ji Tisheng Chengzai Xingneng Cuoshi (in Chinese) [Road and bridge load tests and measures for improving load-bearing performance] [J]. Sichuan Cement, 2025, (05): 246-248. DOI: 10.20198/j.cnki.scsn.2025.05.086.
[4] Li Xiao Yan. Research on Teaching Design and Practice of SolidWorks Application in Secondary Vocational Education Based on Work Process [D]. Guangdong Polytechnic Normal University, 2025. DOI: 10.27729/d.cnki.ggdjs.2025.000005.
[5] Gruyter D. Structural steel design [M]. Walter de Gruyter GmbH & Co KG, 2025.
[6] Long K, Li Z Z. ANSYS 2022 Youxian Yuan Fenxi Cong Rumen Dao Jingtong 9 (in Chinese) [ANSYS 2022 Finite Element Analysis: From Beginner to Expert] [M]. Posts & Telecom press: 202212: 331.
[7] Code for design of the municipal bridge: CJJ 11-2011 [S], 2011.
[8] Jiang X J. Gonglu Qiaoliang Zhuangji Chengzai Liing Zaihe Jiance Fangfa (in Chinese) [Static load testing method for the bearing capacity of highway bridge pile foundations] [J]. Development Guide to Building Materials, 2025, 23(04): 40-42. DOI: 10.16673/j.cnki.jcfzdx.2025.0145.
[9] Lee H A, Park G J. Nonlinear dynamic response topology optimization using the equivalent static loads method [J]. Computer Methods in Applied Mechanics and Engineering, 2015, 283: 956-970.
[10] Liu H W. Gongcheng Lixue (in Chinese) [engineering mechanics] [M]. Beijing: Higher Education Press, 2017: 45-48.
[11] Hu Xiao Lun. Flutter, Buffeting and Aerostatic Stability Analysis for Long-span Cable-stayed Bridges [D]. Tongji University, 2006.
[12] Yi T H, Zheng X, Yang D H, et. Research Advances on Load-carrying Capacity Evaluation Technology of Highway Bridges [J]. China Journal of Highway and Transport, 2025, 38(01): 129-143. DOI: 10.19721/j.cnki.1001-7372.2025.01.009.
[13] Wang X Y. Research on Ancient Bridges in Pingdingshan Area [D]. Henan Universit, 2022. DOI: 10.27114/d.cnki.ghnau.2022.000627.